

$4d^{-1}$ photoelectron spectra and subsequent $N_{4,5}OO$ Auger electron spectra of atomic Sb

M. Patanen,* S. Heinäsmäki, S. Urpelainen, S. Aksela, and H. Aksela

Department of Physics, University of Oulu, Post Office Box 3000, FIN-90014 University of Oulu, Finland

(Received 8 April 2010; published 20 May 2010)

$4d^{-1}$ photoelectron and subsequent $N_{4,5}OO$ Auger electron spectra of Sb have been measured using synchrotron radiation. Features created by an open shell electronic structure of atomic Sb in the spectra have been interpreted using multiconfigurational Dirac-Fock calculations. The results are compared with the molecular Sb_4 and the comparison shows that the relaxation pathways of the hole states in atomic and molecular Sb are very different, so that different groups of states are populated in the corresponding Auger spectra.

DOI: [10.1103/PhysRevA.81.053419](https://doi.org/10.1103/PhysRevA.81.053419)

PACS number(s): 32.80.Fb, 32.80.Hd

I. INTRODUCTION

The electron configuration of antimony in the ground state is $[Kr]4d^{10}5s^25p^3$. The half-filled valence orbital makes antimony a good dopant for semiconductors, and therefore antimony is widely used in industry, for example, in infrared detectors. It is therefore worthwhile to look at the atomic antimony in order to get reference information for the electronic transitions. This means gathering data on relative photoionization intensities, lifetimes of singly ionized states, and Auger decay rates. The comparison of these to the corresponding data on antimony in the form of clusters, solids, and alloys makes it possible to monitor the changes in the electronic structure in great detail. There have been studies of antimony alloys by means of photoelectron spectroscopy, but studies of elemental antimony have been scarce. Pollak *et al.* and Ley *et al.* have studied the Al ($K\alpha$) excited $4d^{-1}$ and valence band photoelectron spectra of elemental Sb in solid form [1,2].

Solid Sb evaporates predominantly as Sb_4 clusters. Therefore, a lot of studies of Sb_4 have been reported recently, including Auger and photoelectron spectroscopies and electron-ion coincidence experiments (see, e.g., [3–5] and references therein). Most of the studies of atomic antimony have been based on the recording of optical transitions (see, e.g., [6–9] for details). Many of the previous studies were made using discharge lamp sources. In this study Sb_4 clusters are thermally fragmented to Sb_2 molecules and further to atoms using a special oven system. In this work we present the $4d^{-1}$ photoelectron spectrum (PES) and the subsequent $N_{4,5}OO$ Auger electron spectrum (AES) of atomic Sb.

II. EXPERIMENTS

Synchrotron radiation from the undulator beamline I411 [10] at the MAX-II storage ring in the MAX-lab was used to ionize the atomic vapor. An inductively heated oven was used to evaporate the solid-phase Sb. Antimony evaporates as Sb_4 molecules, which can be further fragmented to Sb_2 and Sb by strongly increasing the temperature of the upper part of the specially designed oven system [11], but keeping the vapor flow from the reservoir part in control. The oven system (shown in Fig. 1) consists of three parts, which are

separated by graphite decks. Solid Sb powder is placed toward the lowest part of the oven, where it evaporates. The vapor beam (consisting mostly of Sb_4 clusters) heads to the middle and uppermost parts of the oven through the narrow chink between the deck and the wall of the crucible. On their way through the oven the fast Sb_4 clusters collide with the walls of the crucible and with the graphite deck and also with other Sb_4 clusters, and they fragment to Sb_2 and Sb. The heating is focused toward the uppermost part of the oven system, which enhances the kinetic energies of the colliding clusters and makes the collision-induced fragmentation more probable. Finally the Sb vapor flows to the interaction region through a small capillary creating a focused beam of Sb atoms and clusters with an estimated pressure of 10^{-3} mbar. There was no thermometer attached to the oven system and therefore no estimation of the temperature is given. A modified Scienta SES-100 electron energy analyzer [12] was used to record the emitted electrons at the “magic” 54.7° angle with respect to the polarization vector of the horizontally polarized synchrotron radiation, corresponding to the angle-independent measurements. The electron spectrometer is equipped with a resistive anode position-sensitive detection system making possible the gating of electron detection during the short inductive intervals and thus removing the effects of the magnetic fields of the emitted electrons. The energy of the ionizing radiation was 90 eV. In the measurements of the atomic Sb $4d$ PES, an electron analyzer pass energy of 10 eV and a curved entrance slit with a width of 0.8 mm were used. The monochromator exit slit width was 30 μm . The instrumental contribution from the photon bandwidth and the electron analyzer to the linewidths was estimated to be about 40 meV. Doppler broadening was estimated to be less than 20 meV. The PES was calibrated with simultaneously measured Sb_4 $4d$ photolines based on the Xe $4d$ reference lines [3]. The AES was measured with a pass energy of 5 eV, an electron energy analyzer entrance slit width of 0.8 mm, and a beamline exit slit width of 800 μm . The $N_{4,5}OO$ AES was calibrated with Xe $N_{4,5}OO$ AES [13], and the transmission correction to kinetic energies between 7 and 20 eV was also performed using the known intensities of the lines in the Xe $N_{4,5}OO$ AES as a reference. Due to the lack of calibration lines, no transmission correction is made to intensities below 7 eV kinetic energy, which means that the intensities in this region can be strongly overestimated. Also the pass energy of 5 eV used makes a kinetic energy region below 5 eV unreliable.

*minna.patanen@oulu.fi

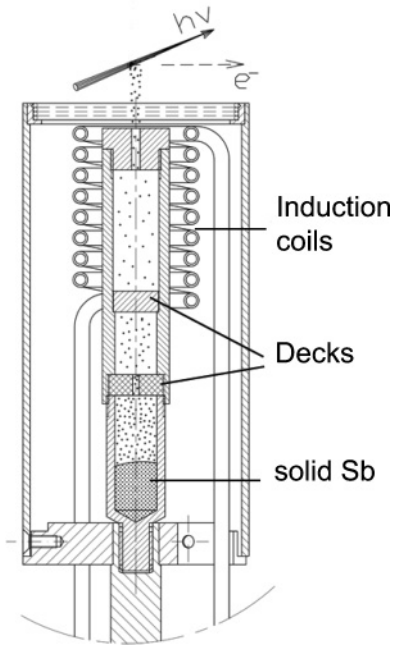


FIG. 1. A schematic picture of the inductively heated oven system used in the experiments.

III. CALCULATIONS

In order to simulate the measured photoelectron and Auger electron spectra, *ab initio* relativistic Dirac-Fock method based calculations were performed. Atomic orbital wave functions were calculated using GRASP92 code [14] and the mixing coefficients and the energies for the states (calculated with the extended average level approximation) were obtained with the GRASP2K package [15]. Photoionization probabilities were approximated using a frozen-core scheme by multiplying the mixing coefficients of the ionic state configuration state functions (CSF) with the corresponding coefficients of their parent CSF in the ground state (the parent being defined as the CSF from which the removal of one electron from the $4d$ orbital gives rise to the ionic CSF) [16]. The energies and transition rates of the Auger transitions were calculated using unpublished routines of the Ratip package [17].

IV. RESULTS AND DISCUSSION

A. $4d$ photoelectron spectrum of Sb

Even though Sb has an open shell structure in the ground state (configuration $[\text{Kr}]4d^{10}5s^25p^3$), only the $4s_{3/2}$ level is populated. The experimental energy difference to the next level is 1.055 eV [6], making the thermal population of the higher levels negligible. Almost pure atomic Sb $4d^{-1}$ PES and comparison to the calculated spectrum are shown in Fig. 2. Notice that there is a small contribution of Sb_2 ($4d_{3/2}^{-1}$ peak) under the peaks labeled as 1, 2, and 3 in Fig. 2. The calculated PES has the same overall shape as the experimental one, but it is slightly wider. The calculated linewidths are a little bit too small. A single nonrelativistic configuration gave a reasonable presentation to the $4d$ ionized state, and implementation of the $5d$ and $6p$ orbitals to the active space did not enhance the results. The experimental spectrum was fitted with the help

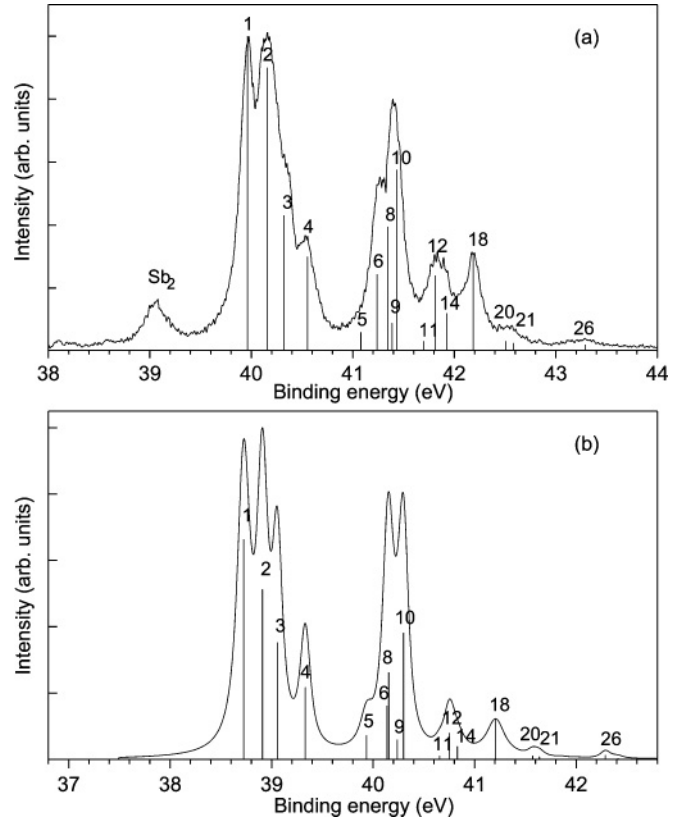


FIG. 2. (a) Experimental atomic antimony $4d$ spectrum. (b) Corresponding calculated PES.

of the calculated $4d^{-1}$ states, and the results are presented in Table I.

B. $N_{4,5}OO$ Auger electron spectrum of Sb

Figure 3(a) shows the raw experimental $N_{4,5}OO$ AES of atomic antimony, and in Fig. 3(b) there is a background-subtracted and transmission-corrected AES. The background subtraction is a rough estimation especially in the low kinetic energy region. Background subtraction has been accomplished by fitting a power function to the data points chosen by a visual estimation and then subtracting pointwise the background data from the raw experimental data. The labels A–D present the possible Auger transitions to the final states: A = $5s^25p^1$, B = $5s^15p^2$, C = $5s^26s^1$, D = $5s^25d^1$. Energy regions are determined using the experimental $4d$ ionization energies and the final state energies from the optical data [9].

Figure 4 presents the experimental $N_{4,5}O_{2,3}O_{2,3}$ AES of atomic antimony and calculated transitions as ticks. The multiconfiguration calculation (MC) with configurations $[\text{Kr}]4d^{10}5s^25p$, $[\text{Kr}]4d^{10}5p^3$, $[\text{Kr}]4d^{10}5s^24f$, $[\text{Kr}]4d^{10}5s^26p$, $[\text{Kr}]4d^{10}5s5p6s$, and $[\text{Kr}]4d^{10}5s5p5d$ was performed. Only two final states are possible for the $N_{4,5}O_{2,3}O_{2,3}$ Auger transition, namely, the $[\text{Kr}]4d^{10}5s^25p_{1/2}$ and $[\text{Kr}]4d^{10}5s^25p_{3/2}$ states, and these states were found to remain very pure in the MC calculation. These states are populated differently by transitions from the different $4d^{-1}$ initial states as is shown in Fig. 4. The number labels without a prime refer to the transitions leading to a $^2P_{1/2}$ final state. The

TABLE I. Binding energies (eV) and relative intensities (relative to the ⁵D₄ peak) of the 4d photoelectron spectrum of Sb. The label refers to Fig. 2. The *LSJ* term of the leading configuration is also shown. Error limits are ±0.05 eV for energies and 15% for intensities.

Label	Configuration	Term	Energy (eV)		Intensity	
			Expt.	Calc.	Expt.	Calc.
1	5p _{1/2} 5p _{3/2} ² 4d _{3/2} ⁴ 4d _{5/2} ⁵	⁵ D ₄	39.99	38.72	0.70	1.29
2	5p _{1/2} 5p _{3/2} ² 4d _{3/2} ⁴ 4d _{5/2} ⁵	⁵ D ₃	0.20	0.19	1.00	1.00
3	5p _{1/2} 5p _{3/2} ¹ 4d _{3/2} ⁴ 4d _{5/2} ⁵	⁵ D ₂	0.38	0.33	0.32	0.69
4	5p _{1/2} 5p _{3/2} ² 4d _{3/2} ⁴ 4d _{5/2} ⁵	³ D ₁	0.60	0.61	0.17	0.42
5	5p _{1/2} 5p _{3/2} ² 4d _{3/2} ⁴ 4d _{5/2} ⁶	⁵ D ₀	1.08	1.21	0.005	0.14
6	5p _{1/2} 5p _{3/2} ² 4d _{3/2} ⁴ 4d _{5/2} ⁶	³ D ₁	1.26	1.41	0.17	0.32
7	5p _{1/2} 5p _{3/2} ² 4d _{3/2} ⁴ 4d _{5/2} ⁵	³ F ₄		1.43		0.02
8	5p _{1/2} 5p _{3/2} ² 4d _{3/2} ⁴ 4d _{5/2} ⁶	⁵ D ₂	1.30	1.43	0.16	0.51
9	5p _{1/2} 5p _{3/2} ¹ 4d _{3/2} ⁴ 4d _{5/2} ⁵	¹ P ₁	1.41	1.51	0.08	0.12
10	5p _{1/2} 5p _{3/2} ² 4d _{3/2} ⁴ 4d _{5/2} ⁶	³ D ₃	1.46	1.57	0.61	0.75
11	5p _{1/2} 5p _{3/2} ² 4d _{3/2} ⁴ 4d _{5/2} ⁵	³ F ₃	1.81	1.93	0.06	0.02
12	5p _{1/2} 5p _{3/2} ² 4d _{3/2} ⁴ 4d _{5/2} ⁵	¹ D ₂	1.88	2.03	0.16	0.16
13	5p _{1/2} 5p _{3/2} ² 4d _{3/2} ⁴ 4d _{5/2} ⁵	¹ S ₀		2.06		0.002
14	5p _{1/2} 5p _{3/2} ² 4d _{3/2} ⁴ 4d _{5/2} ⁵	³ P ₂	1.97	2.11	0.14	0.08
15	5p _{1/2} 5p _{3/2} ² 4d _{3/2} ⁴ 4d _{5/2} ⁵	³ G ₅		2.16		0.000
16	5p _{1/2} 5p _{3/2} ² 4d _{3/2} ⁴ 4d _{5/2} ⁵	¹ G ₄		2.19		0.000
17	5p _{1/2} 5p _{3/2} ² 4d _{3/2} ⁴ 4d _{5/2} ⁵	³ S ₁		2.32		0.002
18	5p _{1/2} 5p _{3/2} ² 4d _{3/2} ⁴ 4d _{5/2} ⁵	³ D ₃	2.23	2.48	0.26	0.24
19	5p _{1/2} 5p _{3/2} ² 4d _{3/2} ⁴ 4d _{5/2} ⁶	¹ S ₀		2.65		0.001
20	5p _{1/2} 5p _{3/2} ² 4d _{3/2} ⁴ 4d _{5/2} ⁶	³ F ₂	2.59	2.85	0.05	0.02
21	5p _{1/2} 5p _{3/2} ² 4d _{3/2} ⁴ 4d _{5/2} ⁶	³ D ₁	2.70	2.91	0.01	0.02
22	5p _{1/2} 5p _{3/2} ² 4d _{3/2} ⁴ 4d _{5/2} ⁵	³ G ₃		3.13		0.000
23	5p _{1/2} 5p _{3/2} ² 4d _{3/2} ⁴ 4d _{5/2} ⁵	³ D ₂		3.14		0.003
24	5p _{1/2} 5p _{3/2} ² 4d _{3/2} ⁴ 4d _{5/2} ⁶	³ F ₃		3.27		0.001
25	5p _{1/2} 5p _{3/2} ² 4d _{3/2} ⁴ 4d _{5/2} ⁶	³ G ₄		3.30		0.000
26	5p _{3/2} ³ 4d _{3/2} ⁴ 4d _{5/2} ⁵	³ D ₃	3.33	3.56	0.09	0.03

numbers with a prime refer to a ²P_{3/2} final state. According to the calculations the Auger decay to the ²P_{3/2} final state gets 54% of the total intensity and the transitions to the ²P_{1/2} final state 46%, respectively. It is remarkable that the most intense transitions originate from the initial states ³D₃, ³P₂, ¹D₂, ¹P₁, ³D₁, and ³D₁ (states 18, 14, 12, 9, 6, and 4 in Table I, respectively), while the transitions from these states to the 5s5p² final states do not play so significant a role. The agreement of the transition energies is good between the experiment and theory; the difference is about 0.2 eV. The theoretically predicted 4d⁻¹ PES is energetically too wide and it is causing the AES to also extend somewhat too much. This is seen, for example, in the theoretically predicted transitions labeled 4 and 6' in Fig. 4 which have too low kinetic energies. The Sb₂ also has corresponding AES in this energy region, and as it is seen in the 4d⁻¹ PES in Fig. 2 there was some Sb₂ left in the vapor beam. Taking into account also the unsatisfactory

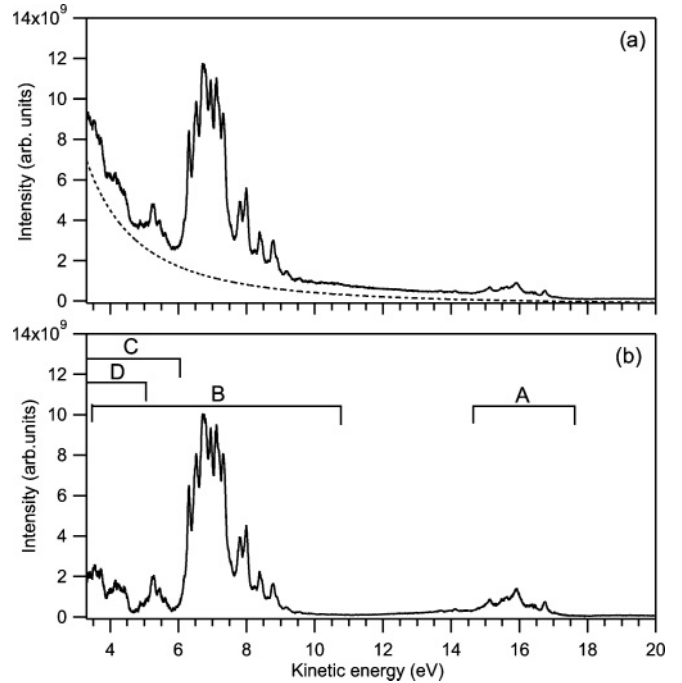


FIG. 3. (a) Raw experimental *N*_{4,5} *O O* AES of atomic antimony. (b) Background subtracted and transmission corrected AES. Labels A–D show the range of the transitions to the final states A = 5s²5p¹, B = 5s¹5p², C = 5s²6s¹, and D = 5s²5d¹ determined using the experimental 4d ionization energies and the final state energies from the optical data [9].

statistic, the interpretation of the *N*_{4,5} *O*_{2,3} *O*_{2,3} AES remains tentative.

In order to theoretically simulate the *N*_{4,5} *O*₁ *O*_{2,3} AES, two sets of calculations were performed. The first calculation was made with only one nonrelativistic final state configuration 5s¹5p² forming eight CSFs. After that, a MC calculation was performed in order to see how the implementation of the 5d and 6s orbitals to the active space affects the

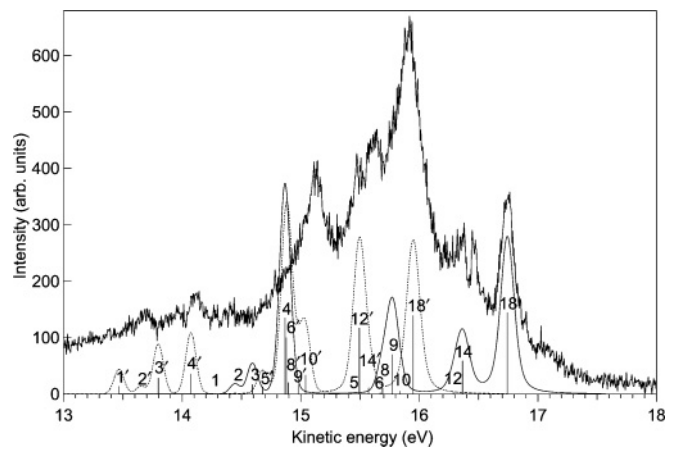


FIG. 4. Experimental *N*_{4,5} *O*_{2,3} *O*_{2,3} AES of atomic antimony and comparison with the MC calculation. The solid line presents the spectrum with the transitions to the ²P_{1/2} final state and the dashed line presents the spectrum with the transitions to the ²P_{3/2} final state. The numbering of the ticks refers to the initial states given in Table I. The ticks are shifted 0.23 eV toward the lower kinetic energies.

TABLE II. Auger final states.

Experiment				Single configuration calculation				Multiconfiguration calculation			
Label	Configuration	<i>LSJ</i> term	ΔE (eV)	Label	Configuration	<i>LSJ</i> term	ΔE (eV)	Label	Configuration	<i>LSJ</i> term	ΔE (eV)
A ^a	$5s5p^2$	$^4P_{1/2}$	0	a	$5s5p^2$	$0.99\ ^4P_{1/2}$	0	a'	$5s5p^2$	$0.98\ ^4P_{1/2}$	0
B ^a	$5s5p^2$	$^4P_{3/2}$	0.370	b	$5s5p^2$	$1.00\ ^4P_{3/2}$	0.337	b'	$5s5p^2$	$0.99\ ^4P_{3/2}$	0.322
C ^a	$5s5p^2$	$^4P_{5/2}$	0.793	c	$5s5p^2$	$0.99\ ^4P_{5/2}$	0.784	c'	$5s5p^2$	$0.97\ ^4P_{5/2}$	0.745
D ^b	$5s5p^2$	$^2D_{3/2}$	2.748	d	$5s5p^2$	$0.99\ ^2D_{3/2}$	4.045	d'	$5s5p^2$	$0.68\ ^2D_{3/2}$	2.709
E ^b	$5s5p^2$	$^2D_{5/2}$	2.905	e	$5s5p^2$	$0.99\ ^2D_{5/2}$	4.199	e'	$5s5p^2$	$0.66\ ^2D_{5/2}$	2.840
F ^b	$5s^26s$	$^2S_{1/2}$	4.784	f	$5s5p^2$	$0.88\ ^2S_{1/2}$	5.945	f'	$5s^26s$	$0.96\ ^2S_{1/2}$	5.029
G ^b	$5s5p^2$	$^2S_{1/2}$	4.842	g	$5s5p^2$	$0.89\ ^2P_{1/2}$	7.288	g'	$5s5p^2$	$0.63\ ^2S_{1/2}$	5.995
H ^b	$5s5p^2$	$^2P_{1/2}$	4.994	h	$5s5p^2$	$0.99\ ^2P_{3/2}$	7.701	h'	$5s^25d$	$0.61\ ^2D_{3/2}$	6.497
I ^b	$5s^25d$	$^2D_{3/2}$	5.512					i'	$5s^25d$	$0.66\ ^2D_{5/2}$	6.636
J ^b	$5s5p^2$	$^2P_{3/2}$	5.663					j'	$5s5p^2$	$0.61\ ^2P_{1/2}$	6.807
K ^b	$5s^25d$	$^2D_{5/2}$	5.706					k'	$5s5p^2$	$0.84\ ^2P_{3/2}$	7.101

^aFrom [8].^bFrom [9].

theoretical spectrum. A set of 55 CSFs constructed by configurations $[\text{Kr}]4d^{10}5s5p^2$, $[\text{Kr}]4d^{10}5s^25d$, $[\text{Kr}]4d^{10}5s^26s$, $[\text{Kr}]4d^{10}5s5d6s$, $[\text{Kr}]4d^{10}5p^25d$, and $[\text{Kr}]4d^{10}5p^26s$ was used in the MC calculation. Table II presents the single-configuration (SC) and MC final states and comparison to the experimental final states obtained from the optical data [8,9]. Even though Sb is a relatively heavy element, the Auger final states can be described well using the *LSJ*-coupling scheme, owing to the fact that the spin-orbit coupling in the final two-hole states is not very strong. It can be seen that the addition of the $5d$ and $6s$ orbitals to the active space does not have so much effect on the final states with multiplicity $2S + 1 = 4$ (a–c in Table II), and it can be seen in Fig. 5 that the transitions to these final states are the most important transitions creating the strongest structures in the AES. One has to notice that due to the uncertainties in the fitting of the weakest peaks of the initial $4d^{-1}$ PES, the fitted Auger spectrum has also great uncertainties especially in the energy range of 7.5–9 eV.

Figure 6 presents comparison between the experimental and the simulated spectra. The calculated spectra have been convolved with a 100 meV Gaussian lineshape to obtain

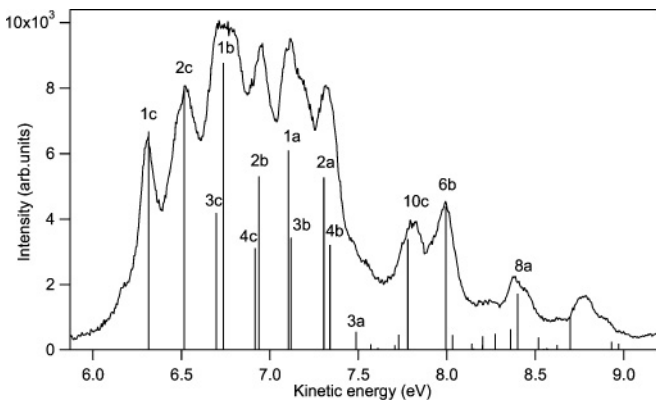


FIG. 5. Experimental $N_{4,5}O_1O_{2,3}$ AES of atomic antimony. Ticks show the energies and intensities of the least-squares method fitted transitions obtained combining the energy difference of the final states from optical data and the initial state energies from the experimental $4d^{-1}$ PES.

better visual comparability. The SC calculation already predicts the features of the $N_{4,5}O_1O_{2,3}$ AES quite well. The kinetic energies of the Auger electrons differ about 1.85 and 2.07 eV from the experimental values in SC and MC calculations, respectively. The MC calculation improves the width of the spectrum slightly. The calculated SC AES is too narrow even though the calculated initial state energy distribution was too broad, which suggests that calculations lack some correlation. In the relative energy region around -0.5 eV the MC calculation begins to create sharp structures, which are transitions to correlating states f'–h' in Table II.

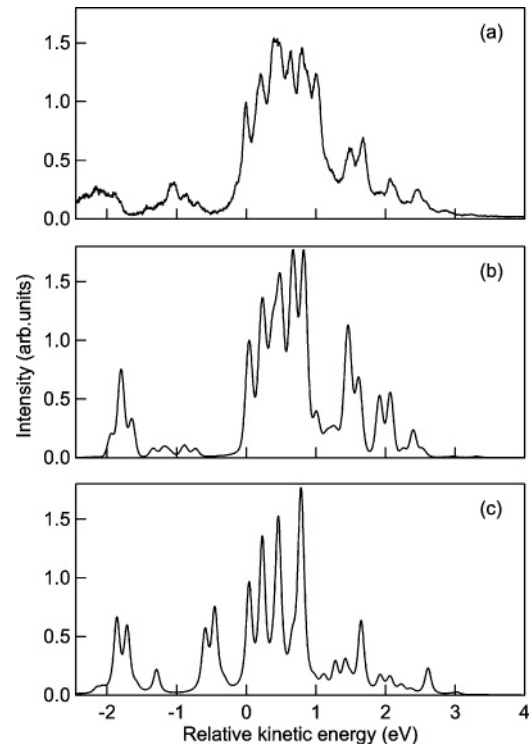


FIG. 6. (a) Experimental $N_{4,5}O_1O_{2,3}$ AES of atomic antimony. (b) Corresponding simulated AES from single-configuration calculation. (c) Corresponding simulated AES from multiconfiguration calculation.

TABLE III. Energies and relative intensities of the strongest $N_{4,5}O_1O_{2,3}$ Auger transitions.

Label	Experimental		SC calc.		MC calc.	
	Energy	Int.	Energy	Int.	Energy	Int.
1c	6.31	0.72	8.16	0.63	8.38	0.62
2c	0.20	0.92	0.18	0.98	0.20	0.87
3c	0.38	0.74	0.33	0.72	0.35	0.10
1b	0.42	1.00	0.45	1.00	0.42	1.00
4c	0.60	0.37	0.61	0.46	0.64	0.04
2b	0.62	0.64	0.63	0.83	0.62	0.18
1a	0.79	0.75	0.78	0.95	0.75	0.97
3b	0.81	0.52	0.78	0.25	0.77	0.33
2a	0.99	0.73	0.97	0.16	0.94	0.04
4b	1.03	0.36	1.05	0.02	1.07	0.04
3a	1.17	0.08	1.12	0.05	1.10	0.04
6c	1.26	0.07	1.41	0.28	1.45	0.02
8c	1.30	0.03	1.43	0.41	1.47	0.04
4a	1.39	0.02	1.39	0.09	1.39	0.17
9c	1.41	0.20	1.51	0.04	1.56	0.01
10c	1.47	0.41	1.57	0.36	1.61	0.46
6b	1.68	0.41	1.86	0.09	1.88	0.05
8b	1.72	0.03	1.88	0.23	1.89	0.07
9b	1.84	0.00	1.96	0.01	1.99	0.00
12c	1.89	0.05	2.03	0.03	2.10	0.01
10b	1.89	0.01	2.02	0.29	2.04	0.09
14c	1.96	0.03	2.11	0.00	2.16	0.01
6a	2.05	0.05	2.19	0.01	2.20	0.02
8a	2.09	0.12	2.21	0.03	2.21	0.02

Compared to the experimental spectrum in the Fig. 6 the MC calculation reproduces better than the SC calculation the intensities in the relative energy range of 3–5 eV.

Table III lists the experimental transitions and the theoretical transitions from the SC and MC calculations. The number in the label refers to the initial state given in Table I and the letter refers to the final state given in Table II. The relative transition energies are quite well reproduced with both calculations, but the agreement of the experimental and calculated intensities varies quite a bit. The strongest transitions labeled as 1a–1c, 2c, and 4c are well reproduced with the SC calculation, but the intensities of the 3c and 4c transitions are heavily underestimated by the MC calculation. Also both calculations almost totally miss the 2a and 4b transitions. The initial states of the Auger transition do not mix with the configurations having 5d and 6s occupations, and the distribution of total intensity to the states having the same initial state does not change. Like in the case of Sb₄ [3] there shake-up transitions might take place during the 4d photoionization. The shake-up electron might remain as spectator during the Auger transition, and the calculations estimate that the energies of the $[\text{Kr}]4d^95s^25p^26p \rightarrow [\text{Kr}]4d^{10}5s5p6p$ transitions overlap with the $N_{4,5}O_1O_{2,3}$ AES. The probability of the monopole shake-up transition during the 4d⁻¹ ionization is about 13%, estimated by calculating the overlap integral of the 5p and 6p radial wave functions and dividing the overlap by the probability that the outermost electrons stay in the initial orbital during the ionization: $|\langle n'_f l_j | n_i l_j \rangle|^2 / |\langle n'_i l_j | n_i l_j \rangle|^2$, where prime stands for the orbital in the final state [18].

C. Comparison between atomic and molecular $N_{4,5}OO$ Auger electron spectra

As was seen in the 4d⁻¹ PES (Fig. 2), the AES probably has some contribution coming from the Sb₂, too. Because the 4d_{3/2}⁻¹ peak of the Sb₂ overlaps with the main structure of the PES of the atomic Sb, and the energy difference to the 4d_{5/2}⁻¹ peak of the Sb₂ is less than 1 eV, it can be assumed that the AES of the atomic and dimer antimony overlap heavily. According to a rule of thumb that the energy difference in the Auger electron kinetic energies of the atom and solid sample is three times the binding energy difference of the corresponding orbital, it can be estimated that the transitions coming from the 4d_{5/2}⁻¹ state have about 3 eV higher kinetic energies than the main transitions in the atomic case. This rule can also be used when comparing the atomic Sb AES with the previously published $N_{4,5}OO$ AES of the Sb₄ [3]. The difference between Sb and Sb₄ intensity weighted average binding energies of the 4d⁻¹ configurations is 1.87 eV [11], which suggests the shift in Auger electron energies to be 5.61 eV. The experimental kinetic energies of the Auger electrons differ, however, much less, namely, about 3 eV, Sb₄ having slightly higher energies and broader structures. The Auger electron energy shift closer to observed 3 eV is obtained when calculating in the case of atomic Sb the new average binding energy including only the main states decaying to the states with 5s¹5p² configurations. By doing this the Auger electron kinetic energy shift of 3.45 eV is obtained.

The final states of the $N_{4,5}OO$ Auger transitions are very differently populated in Sb₄ than in atomic Sb [3]. In the case of Sb₄ the transitions to the final states having one hole in the molecular orbital (MO) with significant contribution of the 5s atomic orbital (AO) and one hole in the MO with significant contribution of the 5p AO are as important as the transitions to the final states having two holes in the MO with significant contribution of 5p AO. In atomic Sb the final states having 5s5p² configuration are much more populated than the states with 5s²5p configuration. This is of course quite natural when counting the number of possible SC final states: in the atomic case there are eight and two states originating from the 5s5p² and 5s²5p configurations, respectively. The calculated intensity ratio between $N_{4,5}O_1O_{2,3}$ and $N_{4,5}O_{2,3}O_{2,3}$ Auger groups is 9:1. In the case of Sb₄ the number of the final states of the allowed Auger transitions can be estimated in the first approximation to be the states that have at least one of the holes in the orbital with the same symmetry as the orbital having the hole in the initial state. The Sb₄ molecule has T_d symmetry, and in this symmetry group the d orbitals in full rotational symmetry group transform as irreducible representations (irreps) a_1 , t_2 , and e . The s-orbital transforms as irreps a_1 and t_2 , and p orbitals as irreps a_1 , t_2 , and e . Therefore, there are ten and nine allowed states with configurations analog to 5s⁻¹5p⁻¹ and 5p⁻² atomic configurations, respectively.

V. CONCLUSIONS

In this work the synchrotron radiation excited 4d⁻¹ photoelectron and subsequent $N_{4,5}OO$ Auger electron spectrum of Sb were reported. The open shell electronic structure of

atomic Sb creates rather complicated spectra which have been interpreted using multiconfigurational Dirac-Fock calculations and previously published optical data of the Auger final states. It was found that despite the complex $4d^{-1}$ PES displaying a lot of transitions, the most intense structures in the $N_{4,5}OO$ AES are created by transitions from the initial states 5D_4 , 5D_3 , 5D_2 , and 3D_1 (configuration $[\text{Kr}]4d^95s^25p^3$) to final states $^4P_{1/2}$, $^4P_{3/2}$, and $^4P_{5/2}$ (configuration $[\text{Kr}]4d^{10}5s^15p^2$). It was also noticed that relative configurations having $5d$ and $6s$ orbitals occupied do not mix with the 4P final states. The comparison to corresponding previously published Sb_4 AES was made and it was noticed that the $N_{4,5}O_1O_{2,3}$ and $N_{4,5}O_{2,3}O_{2,3}$ Auger groups are very differently populated in atomic antimony and the Sb_4 molecule.

The relevance of the present results comes from the need of obtaining accurate data for atomic systems, which could then be used in assigning the features found in larger molecules and clusters. In molecules and clusters one typically finds shifts in binding energies, which can sometimes be accounted for with simple models, but often the spectral features also change drastically. Especially in decay spectra this involves the appearance or disappearance of new groups of states, so

that the energy analysis alone can not be used to interpret the spectral features. The decay spectra of clusters with different numbers of atoms may therefore give a hint about the possible evolution of the relaxation pathways as the system size varies. This is linked, for example, to the changes in the domain of the electronic orbitals and to the appearance of bond-like features in larger systems.

ACKNOWLEDGMENTS

This work has been financially supported by the National Graduate School in Materials Physics, the Research Council for Natural Sciences of the Academy of Finland, the Nordforsk Network, and the European Community Research Infrastructure Action under the FP6 “Structuring the European Research Area” Program (through the Integrated Infrastructure Initiative “Integrating Activity on Synchrotron and Free Electron Laser Science”). We thank Pentti Kovala for his assistance during the mechanical design of the experimental apparatus, the staff of the MAX-laboratory for their assistance during the experiments, and S. Fritzsche for allowing access to unpublished routines of the Ratip package [17].

-
- [1] R. A. Pollak, S. Kowalczyk, L. Ley, and D. A. Shirley, *Phys. Rev. Lett.* **29**, 274 (1971).
- [2] L. Ley, R. A. Pollak, S. P. Kowalczyk, R. McFeely, and D. A. Shirley, *Phys. Rev. B* **8**, 641 (1973).
- [3] S. Urpelainen, A. Caló, L. Partanen, M. Huttula, S. Aksela, H. Aksela, S. Granroth, and E. Kukkk, *Phys. Rev. A* **79**, 023201 (2009).
- [4] S. Urpelainen, A. Caló, L. Partanen, M. Huttula, J. Niskanen, E. Kukkk, S. Aksela, and H. Aksela, *Phys. Rev. A* **80**, 043201 (2009).
- [5] M. Huttula, S.-M. Huttula, S. Urpelainen, L. Partanen, S. Aksela, and H. Aksela, *J. Phys. B* **42**, 235002 (2009).
- [6] F. Hassini, Z. Ben Ahmed, O. Robaux, J. Vergés, and J.-F. Wyart, *J. Opt. Soc. Am. B* **5**, 2060 (1988).
- [7] R. Beigang and J. J. Wynne, *J. Opt. Soc. Am. B* **3**, 949 (1986).
- [8] A. Tauheed, Y. N. Joshi, and E. H. Pinnington, *J. Phys. B* **25**, L561 (1992).
- [9] R. J. Lang, *Phys. Rev.* **35**, 445 (1930).
- [10] M. Bässler *et al.*, *Nucl. Instrum. Methods Phys. A* **469**, 382 (2001).
- [11] S. Aksela, M. Patanen, S. Urpelainen, and H. Aksela (unpublished).
- [12] M. Huttula, S. Heinäsmäki, H. Aksela, and E. Kukkk, *J. Electron Spectrosc. Relat. Phenom.* **156**, 270 (2007).
- [13] A. Kivimäki, L. Pfeiffer, H. Aksela, and S. Aksela, *J. Electron Spectrosc. Relat. Phenom.* **101**, 43 (1999).
- [14] F. A. Parpia, C. F. Fischer, and I. P. Grant, *Comput. Phys. Commun.* **94**, 249 (1995).
- [15] P. Jönsson, X. He, C. F. Fischer, and I. P. Grant, *Comput. Phys. Commun.* **177**, 597 (2007).
- [16] M. Huttula, E. Kukkk, S. Heinäsmäki, M. Jurvansuu, S. Fritzsche, H. Aksela, and S. Aksela, *Phys. Rev. A* **69**, 012702 (2004).
- [17] S. Fritzsche, *J. Electron Spectrosc. Relat. Phenom.* **114**, 1155 (2001).
- [18] K. Jänkälä, J. Schulz, and H. Aksela, *J. Electron Spectrosc. Relat. Phenom.* **161**, 95 (2007).